Impact of Reaction Cross Section on the Unified Description of Fusion Excitation Function

Z. Basrak, Philippe Eudes, V. de La Mota, F. Sébille, Guy Royer

Available online at www.sciencedirect.com

ScienceDirect

Physics Procedia 64 (2015) 120 – 129

Physics Procedia

Scientific Workshop on Nuclear Fission dynamics and the Emission of Prompt Neutrons and Gamma Rays, THEORY-3

Impact of reaction cross section on the unified description of fusion excitation function

Z. Basrak[a,*], P. Eudes[b], V. de la Mota[b], F. Sébille[b], G. Royer[b]

[a]*Ruđer Bošković Institute, P.O.Box 180, 10 000 Zagreb, Croatia*
[b]*SUBATECH, EMN-IN2P3/CNRS-Université de Nantes, B.P. 20 722, 44 307 Nantes cedex 3, France*

Abstract

A systematics of over 300 complete and incomplete fusion cross section data points covering energies beyond the barrier for fusion is presented. Owing to a usual reduction of the fusion cross sections by the total reaction cross sections and an original scaling of energy, a fusion excitation function common to all the data points is established. A universal description of the fusion excitation function relying on basic nuclear concepts is proposed and its dependence on the reaction cross section used for the cross section normalization is discussed. The pioneering empirical model proposed by Bass in 1974 to describe the complete fusion cross sections is rather successful for the incomplete fusion too and provides cross section predictions in satisfactory agreement with the observed universality of the fusion excitation function. The sophisticated microscopic transport DYWAN model not only reproduces the data but also predicts that fusion reaction mechanism disappears due to weakened nuclear stopping power around the Fermi energy.

Peer-review under responsibility of the European Commission, Joint Research Centre – Institute for Reference Materials and Measurements

Keywords: Heavy-ion reactions, Intermediate energies, Fusion excitation function, Vanishing of fusion, Reaction cross sections

1. Introduction

The complex interplay between the one body (nuclear mean field) and the two-body (elementary nucleon-nucleon (NN) collisions) degrees of freedom governs the rich zoo of nuclear reaction mechanisms observed in the transition Fermi-energy region. Understanding the role of these two origins of energy dissipation in the course of heavy-ion reactions (HIR) is a long standing challenge put to nuclear models. Study of the fusion excitation function, both complete (CF) and incomplete (IF), and in particular shedding some light onto conditions of fusion disappearance, may be a useful tool to constrain the ingredients entering theoretical models used to describe HIR in this energy range. The modern dynamical models such as Sky3D by Maruhn et al. (2014), TDHF3D by Simenel (2012) or DYWAN by

* Corresponding author. Tel.: +385-1-456-1169 ; fax: +385-1-468-0239.
E-mail address: basrak@irb.hr, eudes@subatech.in2p3.fr

Peer-review under responsibility of the European Commission, Joint Research Centre – Institute for Reference Materials and Measurements
doi:10.1016/j.phpro.2015.04.016

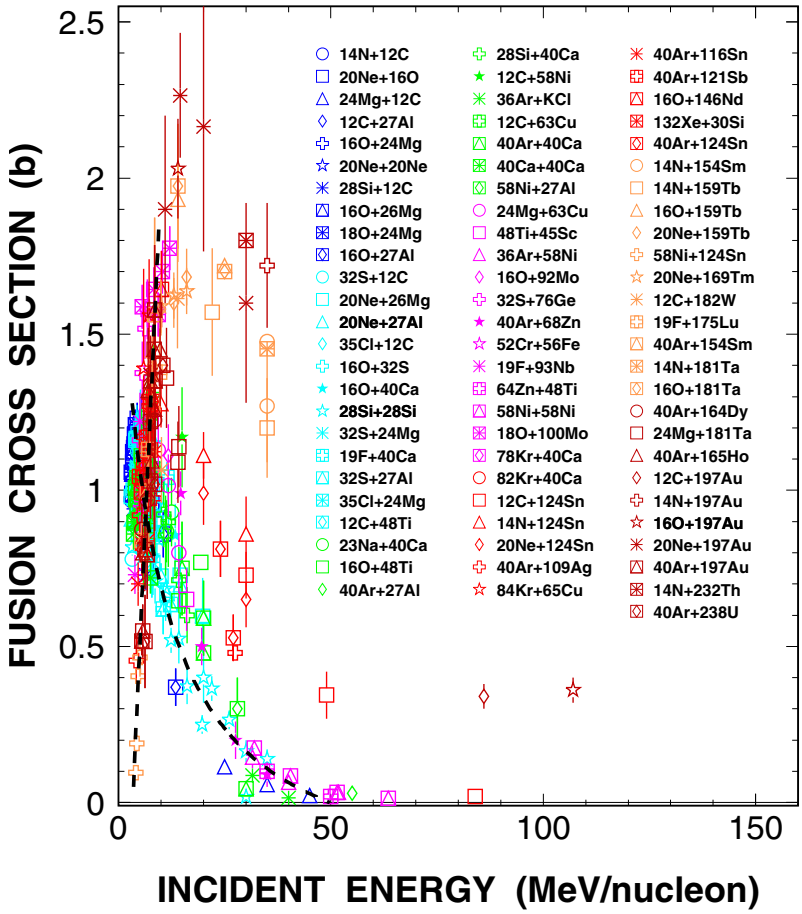

Fig. 1. Raw fusion cross sections σ_f plotted as a function of $E_{\rm inc}$. The inventoried systems are distinguished among them by symbols and a color code. The same symbols and the color code are used in Eudes et al. (2014-a) where an interested reader may find detailed information on energies, σ values, and references to original works. The dashed line and the dashed curve are intended to guide the eye only.

Sébille et al. (2007) offer the promising theoretical frameworks to resolve above questions especially in selecting the most appropriate effective interaction, see e.g. Dutra et al. (2012), and an improved modeling of the NN collisions.

In two recent papers we have presented a systematic study of both CF and IF fusion cross sections σ_f in the incident energy $E_{\rm inc} = E_{\rm lab}/nucleon$ range of $\sim 3A - 155A$ MeV, see Eudes et al. (2013, 2014-a). In total, from the literature published during the past 40 years, we have collected 382 CF and CF+IF σ_f data points belonging to 81 reaction systems with a vast variety of projectile–target pairs, system mass asymmetry, system isospin content as well as in the large range of covered system masses $A_{\rm sys} = 26 - 278$ nucleons.

2. Scaling of fusion cross sections

Discarding those σ_f data points for which we have strong indication that the σ_f value suffers from a non-fusion contribution, cf. in Eudes et al. (2013, 2014-a), or that other reaction mechanism has been erroneously identified as fusion, Eudes et al. (2014-b), one ends with 76 systems and 316 CF+IF σ_f data points. These data, as a function of $E_{\rm inc}$, are displayed in figure 1. Clearly, most of these raw σ_f data points gather in a narrow domain of the σ_f vs $E_{\rm inc}$ plane although the lighter systems (blue, cyan, and green symbols) gather along an arclike structure (see the dashed curve) while the heavier ones (pink, red, and orange symbols) follow a line which sharply rises with $E_{\rm inc}$ (see

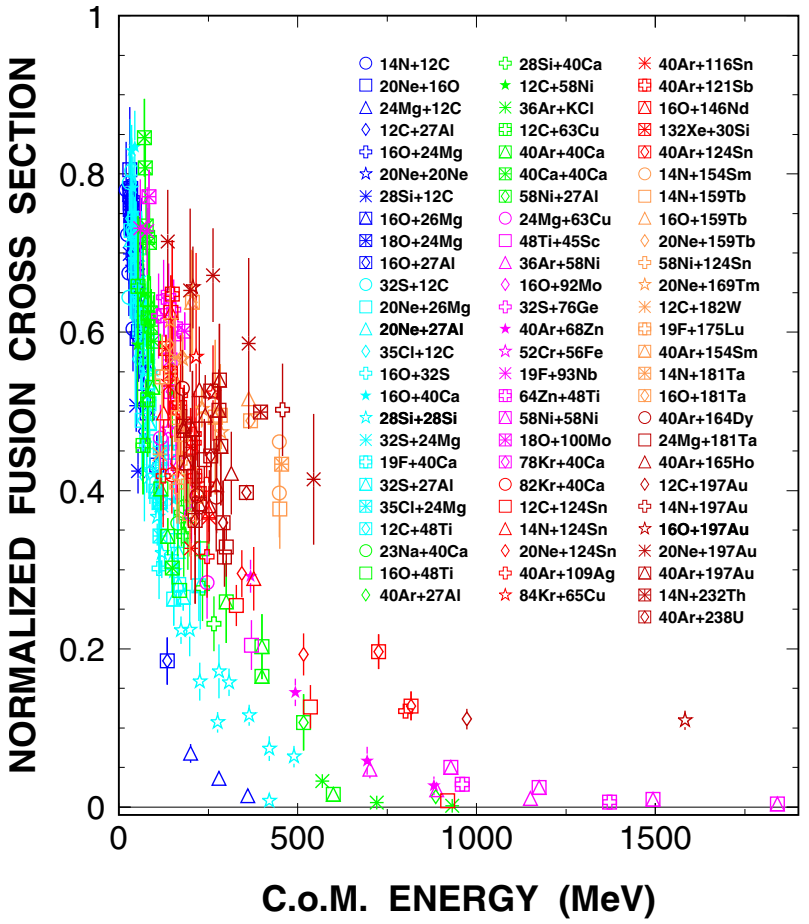

Fig. 2. Normalized fusion cross sections σ_n plotted as a function of $E_{\mathrm{c.m.}}$.

the dashed line). The fact that systems of low and high mass A_{sys} do not fall together is expected due to the known dependence of the fusion cross section on the system size. To remediate it, one normalizes σ_f by the (total) reaction cross section σ_r at the same E_{inc}. The obtained $\sigma_f/\sigma_r = \sigma_n$, as suggested by Lautesse et al. (2006), is in figure 2 plotted as a function of center-of-mass energy $E_{\mathrm{c.m.}} = (E_{\mathrm{lab}}/A_p)\,(A_pA_t/A_{\mathrm{sys}})$, where $A_{\mathrm{sys}} = A_p + A_t$ and A_p (A_t) stands for projectile (target) mass. By the applied normalization, the huge difference between the lighter and the heavy systems in their dependence of the fusion σ_f as a function of increasing energy of figure 1 is completely washed out: All the systems display a similar arclike dependence on energy although it seems that arcs are shifted along abscissae as a function of the increasing A_{sys}. However, a scrutiny scan of the data reveals the true cause of this observed behavior. Systems of distinct arcs do not differ by their A_{sys} but rather by their A_p vs A_t asymmetry. Defining abscissa in units of the so-called system available energy $E_{\mathrm{av}} = E_{\mathrm{c.m.}}/A_{\mathrm{sys}}$ one does express the mass asymmetric systems on the same footing with those which are mass symmetric. The normalized σ_n as a function of E_{av} is displayed in figures 3 and 4. Disregarding for a while discussion of the different panels of these figures, one may draw a general conclusion: By properly reducing σ_f values with σ_r and by applying an original energy scaling, the fusion excitation function, irrespectively of the details of a given reaction system, follows a simple universal law.

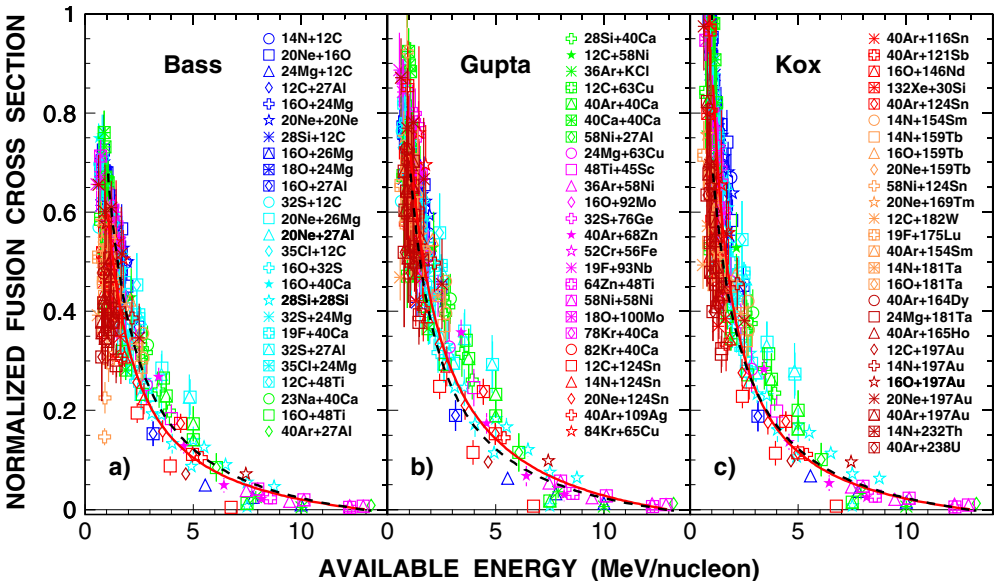

Fig. 3. Normalized fusion cross sections σ_n plotted as a function of $E_{\rm av}$. The σ_r used for normalization is due to a) Bass (1980), b) Gupta and Kailas (1984), and c) Kox et al. (1987), respectively. The full red curve in each panel is due to a fit with the homographic function of Eq. (2), whereas the dashed black curve is due to the same kind of fit of panel c) in figure 4.

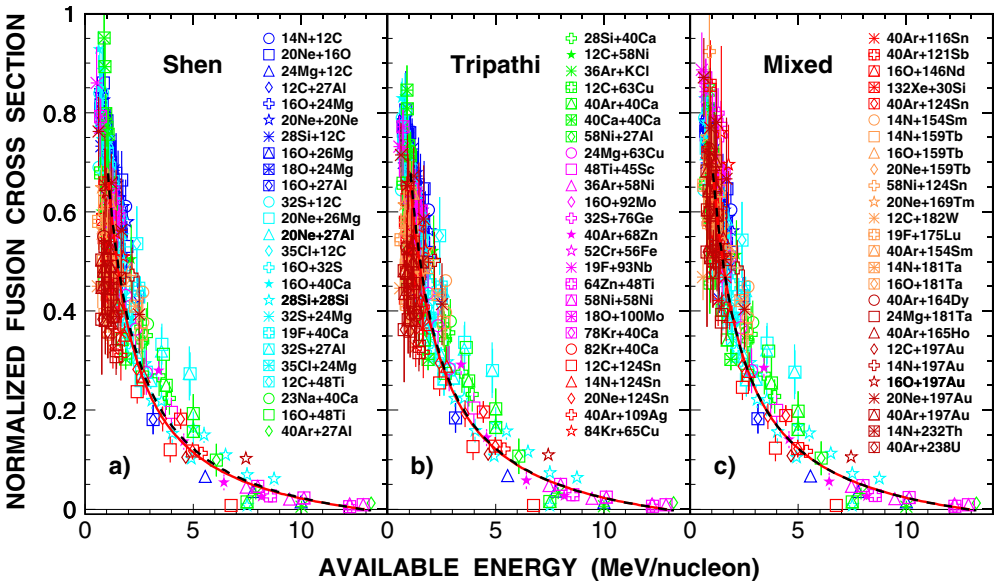

Fig. 4. Normalized fusion cross sections σ_n plotted as a function of $E_{\rm av}$. The σ_r used for the normalization is due to a) Shen et al. (1989), b) Tripathi et al. (1996), and c) the *Mixed* approach (see text for details), respectively. The full red curve in each panel is due to a fit with the homographic function of Eq. (2), whereas the dashed black curve is due to the fit of panel c).

3. Reaction cross section

Besides on experimental uncertainties of σ_f the exact parameter values of the observed universal fusion excitation function are somewhat dependent on the σ_r-values used for the σ_f normalization. In this contribution, we focus on

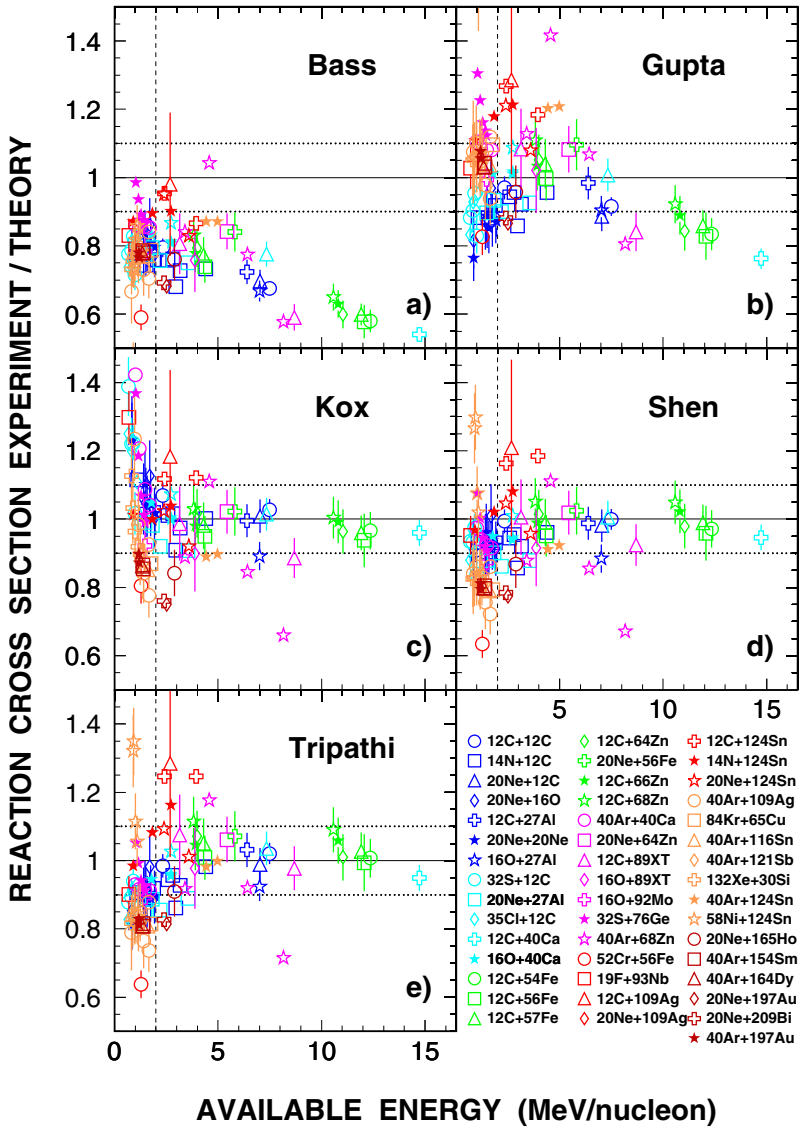

Fig. 5. Ratios of experimental σ_r and theoretical predictions for five models as a function of $E_{\rm av}$. Panels display σ_r ratios with the models of a) Bass (1980), b) Gupta and Kailas (1984), c) Kox et al. (1987), d) Shen et al. (1989), and e) Tripathi et al. (1996). An interested reader may find detailed information on experimental σ_r and references to original works in Eudes et al. (2014-a).

the data normalization problem and the impact of the implemented σ_r. Accurate measurement of the total σ_r is rather hard so that these data are scarce and it would be inappropriate to apply them to the ensemble of the collected σ_f data. Therefore, one commonly resorts to phenomenological approaches to calculate σ_r, a solution which suffers for its own uncertainties and ambiguities. Thus, the uncertainty arising from the use of a particular parameterization of σ_r has to be investigated. Among a number of phenomenological parameterizations of σ_r we have investigated five of them due to Bass (1980); Gupta and Kailas (1984); Kox et al. (1987); Shen et al. (1989); Tripathi et al. (1996), i.e. in this study we have included the pioneer one due to Bass (1980) and the most recent one by Tripathi et al. (1996). All

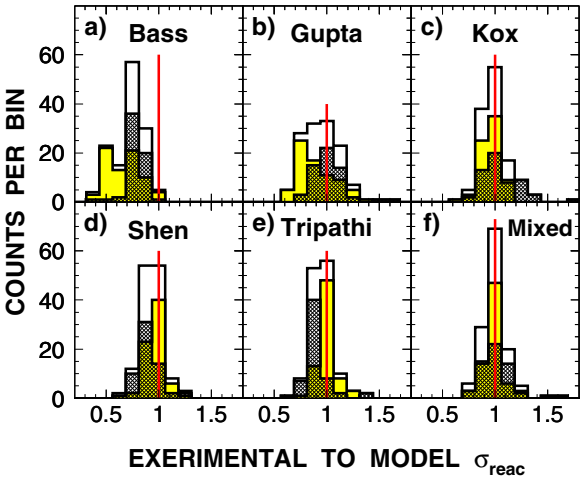

Fig. 6. Histograms of the ratios between the experimental σ_r and the σ_r-values calculated by the models of a) Bass (1980), b) Gupta and Kailas (1984), c) Kox et al. (1987), d) Shen et al. (1989), e) Tripathi et al. (1996) and the *Mixed* one. The yellow and the hashed histograms refer to the projections of the σ_r-ratio values above and below $E_{\rm av} = 2$ MeV/nucleon, respectively.

these approaches rely on the strong absorption picture of nuclear processes and differ among themselves in the way the basic relation

$$\sigma(E) = \pi R^2 (1 - \frac{V}{E}) \tag{1}$$

is parameterized. In Eq. (1), the cross section depends on the inverse of energy E while the radius R and the potential depth V may be, in a first approximation, considered as a constant for a given system. Various models differ in the treatment of R and V by introducing or not a certain dependence on energy and/or on some other system properties, usually A_p or $A_{\rm sys}$, to the one or both of them. In order to infer reliability of each of the models, in figure 5 we compare them with 134 experimental σ_r measured for 46 systems.

From figure 5, one may infer that some of the models, on the average, overpredict σ_r. This conclusion is made plausible by projecting the σ_r-ratio values onto the ordinate of each of the panels. The resulting histograms are shown in figure 6. The hollow histograms display the projections of the full σ_r data set, i.e. at all $E_{\rm av}$. The yellow and the hashed histograms refer to the projections of the σ_r-ratio values above and below $E_{\rm av} = 2$ MeV/nucleon, respectively. Clearly, the Bass approach strongly and the Kox one moderately overpredict the measured σ_r at all $E_{\rm av}$, whereas parameterizations of Eq. (1) by Shen et al. (1989) and by Tripathi et al. (1996) moderately overpredict σ_r for $E_{\rm av} \lesssim 2$ MeV/nucleon and the one by Gupta and Kailas (1984) at energies $E_{\rm av} \gtrsim 2$ MeV/nucleon. By investigating the projection histograms in some detail, we heuristically define the most appropriate combination of model predictions. So, the *Mixed* σ_r is defined as follows

$$\sigma_r(Mixed) = \begin{cases} \sigma_r(Tripathi), & for\ E_{\rm av} < 2\ \text{MeV/nucleon},\ A_{\rm sys} < 86 \\ \sigma_r(Gupta), & for\ E_{\rm av} < 2\ \text{MeV/nucleon},\ A_{\rm sys} \geq 86 \\ \frac{1}{2}[\sigma_r(Tripathi) + \sigma_r(Shen)], & for\ E_{\rm av} \geq 2\ \text{MeV/nucleon},\ all\ A_{\rm sys}. \end{cases}$$

With no doubt, from figure 6, one infers that the heuristic *Mixed* choice for the normalization σ_r reproduces on the best manner the experimental σ_r-values regarding both the centroid and the width of the distribution histogram, see panel f) of figure 6.

Let us discuss figures 3 and 4 in some detail. In figure 3 shown are normalizations with σ_r of Bass, Gupta, and Kox, respectively and in figure 4 those with σ_r of Shen and that of Tripathi as well as the one labeled *Mixed* obtained by a heuristic approach. These plots corroborate the conclusion that the *Mixed* σ_r is the best choice for the normalization of fusion σ_f. It is interesting to note that in figures 3 two of the models violate the normalization condition. In fact, out of the 316 data points in the case of Gupta and that of Kox (panels b) and c) in figures 3, respectively) 2 and 41

points, respectively violate the physically allowed range for the normalized cross section values $\sigma_n = \sigma_f/\sigma_r$, namely between 0 and 1. All these points are due to σ_n overflow that occurs at low energies.

4. Fitting the universal fusion excitation function

Assuming the applicability of the strong absorption concept, in the first approximation both σ_f and σ_r may be expressed by the same functional form given by Eq. (1). Consequently, for the reduced cross section one gets a simple homographic law

$$\sigma_n(E) = \frac{\sigma_f(E)}{\sigma_r(E)} = a + \frac{b}{c+E}, \tag{2}$$

where a, b, and c are free parameters and E is taken as E_{av}, cf. in Eudes et al. (2013, 2014-a). The σ_n data points of each panel of figures 3 and 4 have been fitted with the three-parameters homographic function of Eq. (2). The obtained best fit result is displayed by the red full curve for each σ_n. Interestingly enough, independently of the σ_r chosen for the normalization procedure, the best fit curve gives for the energy of disappearance of the CF+IF fusion process the same value: $E_{\mathrm{av}} = 12.98 \pm 0.06$ MeV/nucleon. Also, at low energy, all the best fit curves overlap. The fit results of different normalization cases disagree by at most about 5 % of σ_n and this occurs at intermediate values of E_{av}. That may be easily inferred by the dashed black curve that is drawn in each panel of figures 3 and 4 and which represents the best fit result in the case of the heuristic (*Mixed*) σ_r. Although the best fit result does not depend strongly on the details of the σ_r parameterization, this subject is open to further investigation. However, the homographic functional law of Eq. (2) seems to be established without any doubt.

5. Predicted fusion cross sections

Theoretical approaches suitable to predict the fusion cross sections well above the fusion barrier are rather scarce. Among the approaches in closed empirical form which is well adjusted for the massive calculation of σ_f we have investigated two models, those by Bass (1974, 1977) and by Matsuse et al. (1982). It has to be mentioned that these models, and in particular the one by Matsuse et al. (1982), have not been tested on a large number of HIR and especially not for the rather vast span of reaction characteristics that the present collection of σ_f data points covers. Anyway, in figures 7 and 8 are presented the σ_f-values predicted by these two models when for the normalization are taken the σ_r-values calculated according to Bass (1980), Kox et al. (1987) and Tripathi et al. (1996). The predictions of Bass (1974, 1977) rather well reproduce the general trend of the excitation function although the σ_n-values for each of the normalizations used overpredict data for $E_{\mathrm{av}} > 8$ MeV/nucleon, cf. in figure 7. Generally speaking, these normalized cross sections split into two more or less distinct branches that overlap at the extreme values of E_{av}. In the calculation of σ_r, the friction parameter of the Bass model has been fixed to the recommended value, i.e. to 5/7. By varying the value of this parameter and/or by introducing an additional degree of liberty into the model one may hope to bring the model prediction to the full homographic universality of the experimental data. In the case of σ_f by Matsuse et al. (1982) the normalized σ_n is almost constant for $E_{\mathrm{av}} > 3$ MeV/nucleon and amounts between 20 % and 27 % of the total reaction σ_r at the highest energy considered, cf. in figure 8. Such a result suggests that the fusion reaction mechanism would be present at any E_{inc}. We mention that with σ_f of Bass (1974, 1977) the normalization condition $0 \le \sigma_n \le 1$ is violated at 9 of 316 points in the case of σ_r by Kox et al. (1987), whereas for σ_f of Matsuse et al. (1982) the normalization is always violated – for 8, 29 and 16 points when σ_r is calculated by Bass (1980), Kox et al. (1987) and Tripathi et al. (1996), respectively.

Another possible way in reproducing fusion excitation function offer various dynamical simulations of HIR. This approach is, however, extremely demanding in the CPU time because the simulation has to be carried out at a number of the reaction impact parameters in fine step and at each energy under study. That is why these models have essentially been used to qualitatively study the phenomenon of heavy-ion fusion while the rare example of the published quantitative studies of fusion excitation function by microscopic transport theories are with the BUU model by Xu et al. (1990), the Landau-Vlasov (LV) model by Eudes et al. (2013), the SMF model by Shvedov et al. (2010) and the DYWAN model by Eudes et al. (2013). The BUU and LV models completely fails in reproducing both absolute values and trends of our universal fusion excitation function given by the homographic law of Eq. (2), cf. in Eudes

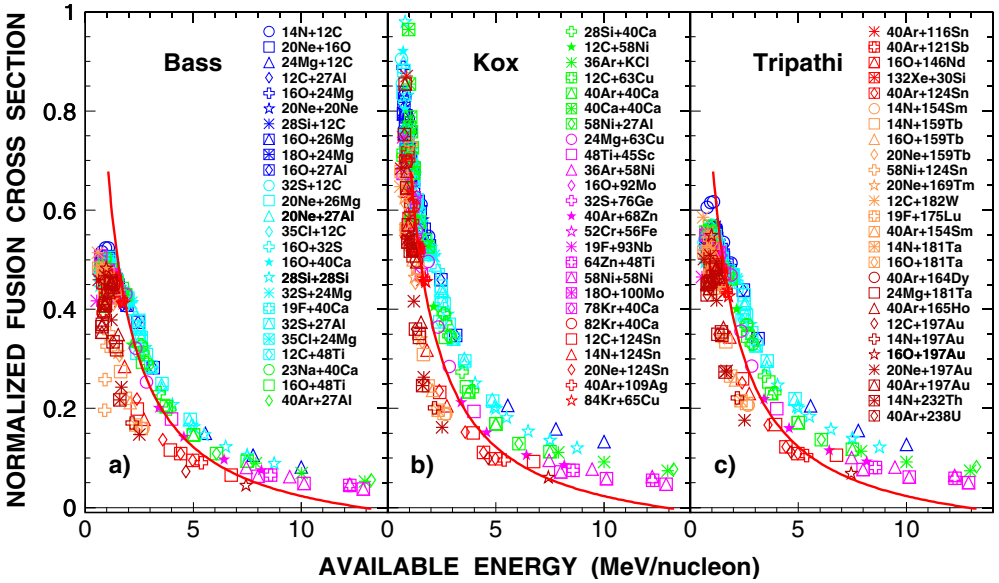

Fig. 7. The predicted σ_f by the Bass (1974, 1977) model for the data points of figures 1 and which are normalized by σ_r calculated with a) Bass (1980), b) Kox et al. (1987) and c) Tripathi et al. (1996) models. To guide the eye in each panel is plotted the best fit curve of panel c) of figure 4.

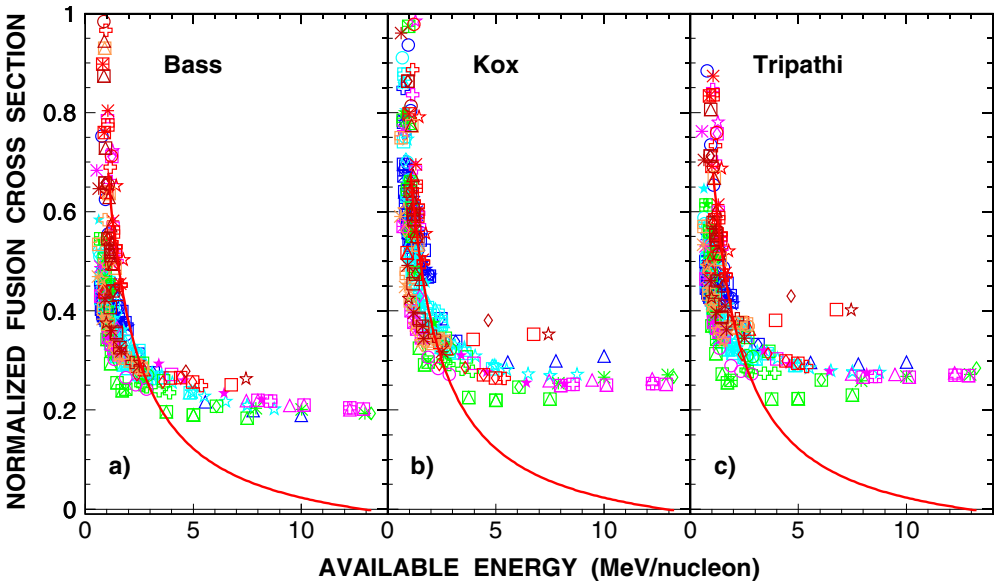

Fig. 8. Same as figures 7 but here the σ_f values are predicted by the model of Matsuse et al. (1982).

et al. (2013). The SMF model is quite successful but only two points for the ^{36}Ar + ^{96}Zr system are published so far, see in Shvedov et al. (2010) and Eudes et al. (2013). The predictions of the DYWAN model are shown in figure 9 by the filled circles (^{36}Ar + ^{36}Ar), triangles (^{36}Ar + ^{58}Ni) and reversed triangles (^{58}Ni + ^{58}Ni). The DYWAN model for $E_{\rm av} > 3.5$ MeV/nucleon nicely reproduces both absolute values and fusion excitation function trends, including the energy of fusion vanishing, in the full accordance with the established universal homographic law. Moreover, this model suggests that the fusion reaction mechanism ceases to exist due to the insufficient stopping power of HIR around the Fermi energy owing to a longer mean free path caused by the interplay between a weakened nuclear mean

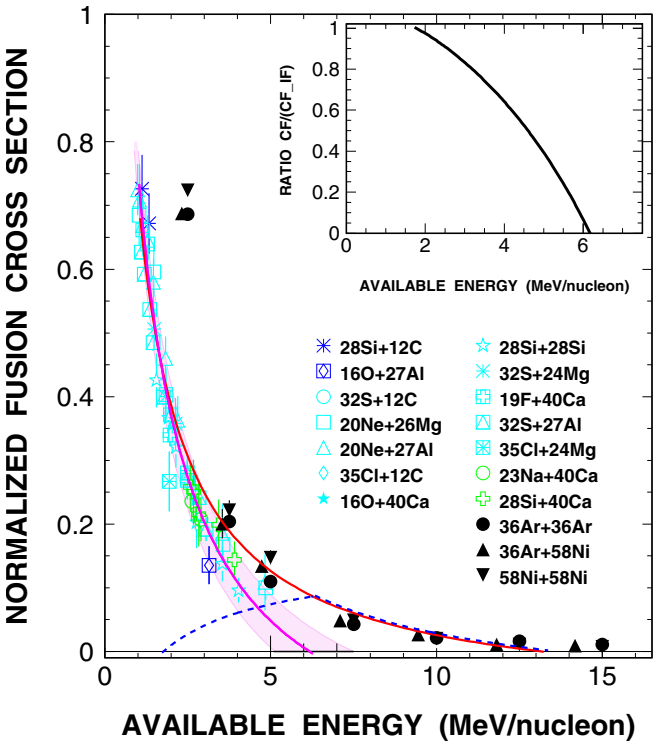

Fig. 9. Normalized complete fusion cross sections σ_n as a function of $E_{\rm av}$ from those measurements which have reported data on both complete and incomplete fusion. The full violet curve is due to the best fit by the homographic function of Eq. (2). The light-violet background band around the best fit curve is due to the errors on the fit parameters. The full red curve in the main panel is due to the same kind of fit to CF+IF data of the *Mixed* σ_n, in fact, the best fit curve of panel c) of figure 4. The dashed blue curve is the difference of both fusion excitation functions. The open symbols refer to the 14 systems studied experimentally. An interested reader may find detailed information on energies, σ_f-values, and references to original works in Eudes et al. (2014-a). The black filled symbols are result of σ_f as predicted by the DYWAN model of Sébille et al. (2007). The inset displays the ratio of CF and CF+IF best-fit excitation functions as a function of $E_{\rm av}$.

field and a still insufficient stopping efficiency of NN collisions, cf. in Eudes et al. (2013). The phenomenon of the nuclear (pseudo)transparency has been predicted for HIR in the Fermi-energy range a long time ago, see Eudes et al. (1997); Basrak (2004); Novosel et al. (2005), but it received only recently an experimental confirmation, see Lehaut et al. (2010).

6. Complete and incomplete fusion cross section

Only twelve experiments have explicitly been designed to measure both complete and incomplete fusion components, cf. in Eudes et al. (2013, 2014-a). These 57 CF σ_n data points belonging to the 14 reaction systems and obtained with the heuristic σ_r discussed above are displayed in figure 9 as a function of $E_{\rm av}$. The same homographic law of Eq. (2) used in fitting the CF+IF data is here used to obtain the best fit result to the CF data. It is shown by the full violet curve. The used fitting code by James and Roos (1975) provides an uncertainty on the fit parameters a, b, and c. These uncertainties define the light-violet background drawn around the best fit curve. Owing to the rather large experimental error bars and the relatively small number of data points the energy of CF disappearance is not very accurately defined. It reads $E_{\rm av} = 6.2\,^{+1.3}_{-1.1}$ MeV/nucleon. Similarly, CF data display a stronger dependence on the normalization σ_r used. However, the deduced energy of CF disappearance for each of the σ_r used lays well within the above stated uncertainty limits.

In figure 9 by the full red curve is shown the best fit result with the heuristic (*Mixed*) σ_r of panel c) of figure 4. Making difference of the violet CF and the red CF+IF best fit homographic functions allows to infer the main proper-

ties of the incomplete fusion excitation function: IF process opens around $E_{\rm av} \approx 1.5$ MeV/nucleon, reaches maximal value at the energy of CF disappearance ($E_{\rm av} \approx 6$ MeV/nucleon), and vanishes at $E_{\rm av} \approx 13$ MeV/nucleon. An inset displays how the best-fit CF excitation function decreases relatively to the CF+IF one, an observable which has been investigated a long time ago by Morgenstern et al. (1984) who have concluded that the mass asymmetry has a strong influence on the onset of incomplete fusion and on the limiting energy of complete fusion.

7. Conclusions

To summarize, the scrutiny of the existing fusion cross sections well above the reaction barrier allowed us to establish a universal dependence of these data on energy. The established homographic functional description of both the complete and the complete plus incomplete fusion excitation functions is rather stable and the inferred global features of these excitation functions quite weakly depend on the details of the reaction cross section used for data normalization. Nevertheless, the normalization may be improved if additional high quality measurements on both fusion and reaction cross section would be available. The universality of the obtained fusion excitation functions offers an easily applicable check on the reliability of nuclear models. It comes out that the old and rather simple empirical model developed by Bass (1974) which is relying on the concepts of the strong nuclear absorption quite well reproduces the CF+IF fusion excitation function, although the model has been developed to describe the CF only. Most of the much more sophisticated dynamical models fails to reproduce the observed features of fusion. Among these approaches, so far, only the DYWAN model of Sébille et al. (2007) has been able to provide a convincing result in interpreting fusion cross sections.

References

Basrak, Z., 2004. Nucl. Phys. A **738**, 463.
Bass, R., 1974. Nucl. Phys. A **231**, 45.
Bass, R., 1977. Phys. Rev. Lett. **39**, 265.
Bass, R., 1980. *Nuclear Reactions with Heavy Ions*. Springer, Berlin,
Dutra, M., et al., 2012. Phys. Rev. C **85**, 035201.
Eudes, P., et al., 1997. Phys. Rev. C **56**, 2003.
Eudes, P., et al., 2013. Europhys. Lett. **104**, 22001.
Eudes, P., et al., 2014-a. Phys. Rev. C **90**, 034609.
Eudes, P., et al., 2014-b. Nucl. Phys. A **930**, 131.
Gupta, S.K., Kailas, S., 1984. Z. Phys. A **317**, 75.
James, F., Roos, M., 1975. Comput. Phys. Commun. **10**, 343.
Kox, S., et al., 1987. Phys. Rev. C **35**, 1678.
Lautesse, P., et al., 2006. Eur. Phys. J. A **27**, 349 (2006).
Lehaut, G., et al., 2010. Phys. Rev. Lett. **104**, 232701.
Maruhn, J.A., et al., 2014. Comput. Phys. Commun. **185**, 2195.
Matsuse, T., et al., 1982. Phys. Rev. C **26**, 2338.
Morgenstern, H., et al., 1984. Phys. Rev. Lett. **52**, 1104.
Novosel, I., et al., 2005. Phys. Lett. B **625**, 26.
Sébille, F., et al., 2007. Phys. Rev. C **76**, 024603.
Shen, W., et al., 1989. Nucl. Phys. A **491**, 130.
Shvedov, L., et al., 2010. Phys. Rev. C, **81**, 054605.
Simenel, C., 2012. Eur. Phys. J. A **48**, 152.
Tripathi, R.K., Cucinotta, F.A., Wilson, J.W., 1996. Nucl. Instr. Meth. Phys. Res. B **117**, 347.
Xu, H.M., et al., 1990. Phys. Rev. Lett., **65**, 843.